Res Chem Intermed (2015) 41:9295–9306
DOI 10.1007/s11164-015-1999-0

Influence of the carrier and composition of active phase on physicochemical and catalytic properties of CuAg/oxide catalysts for selective hydrogenolysis of glycerol

K. Samson[1] · A. Żelazny[1] · R. Grabowski[1] · M. Ruggiero-Mikołajczyk[1] · M. Śliwa[1] · K. Pamin[1] · A. Kornas[1] · M. Lachowska[2]

Received: 27 October 2014 / Accepted: 3 March 2015 / Published online: 1 April 2015

Abstract The aim of the present study is to investigate the influence of the support and composition of the active bimetallic phase on both the physicochemical and catalytic properties of catalysts for use in glycerol hydrogenolysis reaction. Two series of catalysts with different amounts of copper oxide and/or silver supported on Al_2O_3 or TiO_2 oxides were prepared. To determine the physicochemical properties of the catalysts, the following techniques were used: Brunauer–Emmett–Teller, reactive N_2O adsorption, X-ray diffraction, and temperature-programmed reduction TPR-H_2. Physicochemical characterization revealed that addition of silver modifies the redox properties of the catalysts containing copper oxide and influences their specific surface area. It was found that the type of carrier determines the catalytic activity and selectivities for desired products, strongly influencing their distribution. The Al_2O_3-supported catalysts were much more selective for 1,2-propanediol, whereas 1-propanol was the main reaction product for the titania-supported catalysts. The best catalysts (6Cu/Al and 2Cu/Ti) achieved 38 % glycerol conversion with 71 % selectivity for 1,2-propanediol and 44 % conversion with 62 % selectivity for 1-propanol, respectively.

Keywords Glycerol · Hydrogenolysis of glycerol · $CuAg/Al_2O_3$ · $CuAg/TiO_2$

✉ K. Samson
ncsamson@cyf-kr.edu.pl

[1] Jerzy Haber Institute of Catalysis and Surface Chemistry, Polish Academy of Sciences, ul. Niezapominajek 8, 30-239 Krakow, Poland

[2] Institute of Chemical Engineering, Polish Academy of Sciences, ul. Bałtycka 5, 44-100 Gliwice, Poland

Introduction

In recent years, biodiesel production has increased very sharply. This has been caused by many factors, including diminishing sources of fossil fuels. This increase in biodiesel production is accompanied by an increase in production of glycerol, which is a main byproduct of biodiesel production [1]. Biodiesel is produced by trans-esterification reaction of fats, which co-generates 1 mol of glycerol per 3 mol of synthesized esters, approximately 10 wt % of the total product. This results in a large quantity of glycerol available for conversion. All of this has resulted in an oversupply of glycerol and a drastic drop in its market price [2]. As a consequence, glycerol is considered one of the most important compounds in conversion of biomass-derived feedstock to value-added chemicals [3, 4]. Due to decreasing fossil fuel resources and increasing air pollution, effective utilization of glycerol as a renewable resource by conversion into value-added chemicals is essential [4].

Among value-added chemicals, propylene glycol (PG) is a major commodity that is widely used as a biodegradable functional fluid, e.g., as a de-icing reagent, antifreeze, coolant, and precursor in syntheses of unsaturated polyester resins [5–7]. The conventional method for PG production from petroleum derivatives is expensive and environmentally unfriendly, so its production from renewable resources is highly desired [8].

Glycerol hydrogenolysis is one of the reactions which can be applied to obtain value-added chemicals. This reaction (Scheme 1) is considered as a two- or three-step reaction, depending on the acido-basic conditions: (1) dehydration of glycerol to acetol in the first step, followed by hydrogenation of intermediate in the second step to 1,2-propanediol [10], or (2) dehydrogenation to glyceraldehydes, followed by dehydration to 2-hydroxyacrolein and hydrogenation to desired propanediol [9, 10].

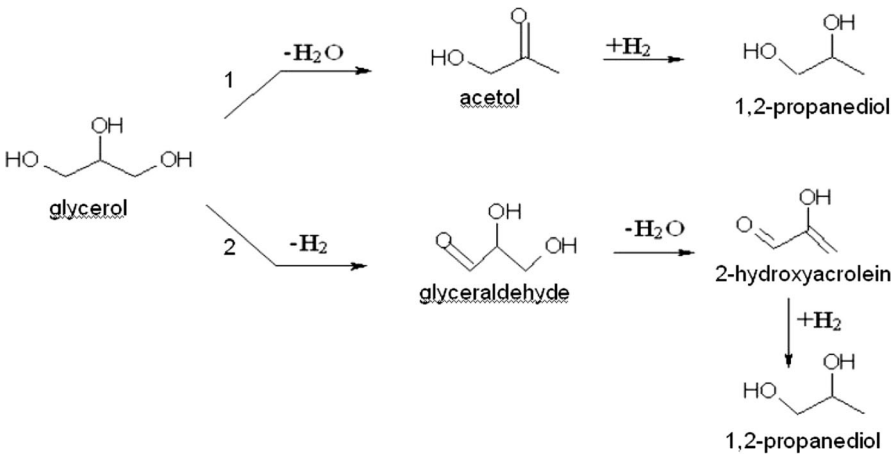

Scheme 1 Glycerol reaction pathways in acidic (*1*) and basic (*2*) reaction conditions

For this reason, use of bifunctional catalyst, possessing both acidic and redox centers, is required. Acidic centers are responsible for glycerol dehydration, while redox centers take part in the second stage, i.e., hydrogenation of acetol to PG [11].

So far, two kinds of catalysts for glycerol hydrogenolysis have been reported in the literature: supported noble-metal catalysts and catalysts containing transition-metal oxides [4]. Noble-metal-based catalysts exhibit high activity in glycerol hydrogenolysis reaction, but their selectivity for 1,2-propanediol is low [10]. Another disadvantage of noble-metal catalysts is their high cost. On the contrary, transition-metal catalysts are cheap and offer much greater selectivity for 1,2-propanediol (even close to 100 %), but the glycerol conversion is limited and requires severe reaction conditions [2]. Most transition-metal catalysts contain copper, as it is known to be an effective catalyst in glycerol hydrogenolysis to 1,2-propanediol by selective cleavage of C–O bond instead of C–C bond [12]. Zhou et al. [4] found that silver addition increases the activity of Cu/Al_2O_3. They also studied the activity of Ag/Al_2O_3 catalysts which did not contain copper, allowing the achievement of 46 % glycerol conversion and 96 % selectivity for 1,2-propanediol [13]. The present work focuses on investigation of the activity of catalysts containing copper, silver or both, deposited on titania and acidic alumina, in glycerol hydrogenolysis reaction. The influence of the support and the composition of the active phase was also investigated.

Experimental

Preparation of catalysts

Mixed CuAg catalysts with varying Cu and Ag contents (see Tables 1, 2 for details) were prepared by a wet impregnation method using aqueous solutions of copper and silver nitrate (Sigma Aldrich and POCh., p.p.a., respectively). Commercial Al_2O_3 (Fluka, acidic, $S_{SA} = 172$ m^2/g) and TiO_2 (anatase tioxide, batch NP 93/205, with traces of SO_4 by XPS analysis, $S_{SA} = 94$ m^2/g) were used as supports (Al and Ti, respectively, hereinafter). The synthesis of the catalysts included evaporation of the

Table 1 CuAg/Al series and their physicochemical characterization

Sample, mmolCummolAg/1 g Al_2O_3	S_{SA}^a (m^2/g)	Porosity[a]		Cu^b metal area (m^2/g)	Copper particle size[b] (nm)
		Total pore volume (mL/g)	Pore size (Å)		
Al	172.3	0.27	38.5	–	–
6Cu/Al	111.9	0.18	38.7	1.0	225.8
2Cu/Al	138.6	0.21	38.6	0.9	81.7
1.5Cu0.5Ag/Al	134.0	0.21	38.5	2.2	26.5
0.5Cu1.5Ag/Al	123.5	0.19	38.5	2.5	15.4
2Ag/Al	124.6	0.18	38.4	–	–

Table 2 CuAg/Ti series and their physicochemical characterization

Sample, mmolCummolAg/1 g TiO_2	S_{SA}^{a} (m^2/g)	Porosity[a]		Cu^{b} metal area (m^2/g)	Copper particle size[b] (nm)
		Total pore volume (mL/g)	Pore size (Å)		
Ti	94.0	0.45	65.9	–	–
6Cu/Ti	59.2	0.24	66.0	9.3	24.5
2Cu/Ti	82.0	0.27	66.1	8.0	9.4
1.5Cu0.5Ag/Ti	73.3	0.30	66.2	0.8	68.6
0.5Cu1.5Ag/Ti	44.6	0.29	67.4	0.2	165.2
2Ag/Ti	38.6	0.26	33.2	–	–

[a] Measured by BET/Barrett–Joyner–Halenda (BJH) method

[b] Measured by dissociative N_2O adsorption

solvent, followed by drying for 10 h at 120 °C and calcination under air flow for 5 h at 350 °C.

Physicochemical characterization of prepared catalysts

The prepared catalysts were characterized by determining their surface area and porosity (BET/BJH method), the active surface of Cu using the method of reactive adsorption of N_2O, the phase composition by XRD, and reducibility by the temperature-programmed reduction (TPR-H_2) method.

Specific surface area and porosity by BET/BJH method

The specific surface area (S_{SA}) and porosity of the oxide supports and synthesized catalysts were determined by the BET method using an Autosorb-1 Quantachrome apparatus, with nitrogen as adsorbate at 77 K. Prior to the measurements, the samples were preheated and degassed under vacuum at 393 K for 18 h. The micropore area was obtained by t-micropore analysis, while the pore size distribution was calculated by the BJH method.

Active surface of copper

The active surface of copper of the fresh catalysts was determined via reactive adsorption of N_2O at 363 K according to the method described in Ref. [14]. The measurements were carried out in a quartz flow microreactor. Approximately 0.25 g of catalyst was reduced at 523 K during 2 h and cooled to 363 K. Then, 100-µl N_2O pulses were injected until the reaction was complete. The amount of reacted N_2O was determined using a mass spectrometer (VG/Fison Quartz 200D). It was assumed in the calculations that reoxidation of the surface copper follows the equation $2Cu(s) + N_2O(g) = Cu_2O(s) + N_2(g)$ and that 1 m^2 of elemental copper corresponds to 6.1 µmol O_2.

X-ray diffraction (XRD) measurements

Diffraction patterns of the supports and prepared catalysts were collected using an X'PERT PRO MPD diffractometer working in Bragg–Brentano geometry. Cu K_α radiation ($\lambda = 1.54178$ Å), a graphite monochromator of the secondary beam (PW3122/00), and an X'CELERATOR detector were used. Measurements (at 40 kV and 30 mA) were performed in the 2θ range from 5° to 90° with interpolated step size of 0.02°. The patterns were recorded at room temperature.

Reducibility by TPR-H_2 method

TPR-H_2 profiles of the catalysts were obtained using a U-shaped quartz flow reactor (diameter ca. 5 mm) in the temperature range of 20–600 °C. About 0.025 g of sample was used for TPR measurements. A mixture of 5 % H_2 in Ar was used as reducing agent. Before TPR analysis, all samples were kept in a helium stream at 373 K for 1.5 h to remove physically adsorbed water. Subsequently, each sample was cooled down to ambient temperature, and TPR analysis was performed with a temperature ramp of 10 °C/min and a flow rate of H_2 + Ar reducing mixture of 30 cm^3/min. The TPR profiles were recorded using a thermal conductivity detector (TCD).

Catalytic activity measurements

Glycerol hydrogenolysis reaction was carried out in a 100-mL PARR batch stainless-steel reactor with mechanical stirring and electronic temperature controller. For a conventional run, 30 mL of 50 v/v % aqueous solution of glycerol (Sigma-Aldrich, p.p.a.) and 2 g of catalyst were used. The typical conditions for a hydrogenolysis test were: pre-reduction of each catalyst ($T = 200$ °C, $p_{H2} = 2$ atm, $t = 2$ h, 100 rpm) and proper hydrogenolysis reaction ($T = 200$ °C, $p_{H2} = 40$ atm, $t = 24$ h, 400 rpm). The liquid and gas products of the reaction were analyzed by HP gas chromatograph (GC) using a flame ionization detector (FID). Only traces (below 5 %) of methane and CO_x—the only gaseous products—were detected. Analysis of liquid products was carried out by the *n*-butanol internal standard method.

Glycerol conversion was calculated according to the following equation: conversion of glycerol [%] = [moles of glycerol consumed/moles of glycerol initially charged] × 100.

Product selectivities were calculated as carbon selectivity according to the following equation: selectivity [%] = [moles of carbon in specific product/moles of carbon in all detected products] × 100.

Results and discussion

Physicochemical characterization of the catalysts

Acidity of supports, their specific surface area and porosity determined by BET/BJH method, and active surface of copper

Quantitative pyridine sorption experiments for Al_2O_3 and TiO_2 oxides were performed using the procedure described in Ref. [15]. No Brønsted acidity was detected, but the concentration and strength of Lewis acid sites (LAS) were different, depending on the support used. The Al_2O_3 support was characterized by possessing a major amount of LAS (0.58 μmol/m^2) with considerably (nearly twice, 0.9) higher strength than for TiO_2 (0.32 and 0.5, respectively). Tables 1 and 2 present lists of prepared catalysts supported on Al_2O_3 and TiO_2, respectively, their specific surface area and porosity obtained by the BET/BJH method, and cupric metal area calculated from dissociative N_2O adsorption.

For both the CuAg/Al and CuAg/Ti series, the specific surface area of the catalysts, S_{SA}, was lower than that of the pure Al_2O_3 and TiO_2 supports. The presence of the copper active phase, as well as the silver addition, led to a decrease of S_{SA}; this effect is particularly visible for the CuAg/Ti series. A decrease in the specific surface area of the support after deposition of active copper or silver phases has frequently been observed in supported metal catalysts [16] and may be due to sintering of the support in the presence of deposited phase or blocking of the support pores, especially by addition of silver. The texture of the CuAg/Al catalysts was similar, with both specific surface area and porosity having comparable values. The surface areas of the CuAg/Ti catalysts were much lower (39–94 m^2/g) and the pore sizes were larger ($\sim$65 Å) than for the CuAg/Al series (112–172 m^2/g and $\sim$38 Å, respectively). The active copper surface, as determined by reactive adsorption of N_2O, depended on the Cu loading and the support used (Tables 1, 2). The copper surface area for the catalysts supported on Al_2O_3 varied in the range from 0.9 to 2.5 m^2/g, while for the catalysts supported on TiO_2 it varied across a broader range, i.e., from 0.2 to 9.3 m^2/g. For both series there was no clear correlation between copper content and active copper surface area. However, as can be seen from Tables 1 and 2, for the studied catalysts, the smaller copper particle size resulted in higher values of copper surface area for the measured samples. In both series, for the catalysts containing only copper, the Cu metal area was almost the same, irrespective of the copper content (2 or 6 mmol). It should be noted that, in Cu metal surface area measurements, the catalysts were reduced at 250 °C, therefore only easily reducible copper is reduced, as emerges from the TPR profiles (see "Reducibility by TPR-H_2 method" section for details). In view of the reaction temperature (200 °C) at which glycerol hydrogenolysis is conducted, only this type of copper is responsible for glycerol conversion or catalytic activity.

X-ray diffraction (XRD) measurements

X-ray diffraction (XRD) analysis was used to determine the phase composition of the obtained samples; Figs. 1 and 2 show the XRD patterns for the CuAg/Al and CuAg/Ti systems, respectively.

For both series of catalysts, it was found that, at high copper content (≥1.5 mmol of Cu), copper was present in the form of copper oxide CuO. For the catalysts containing small amounts of copper (0.5Cu1.5Ag/Al and 0.5Cu1.5Ag/Ti), no patterns related to presence of copper were recorded. A similar effect was observed by Zhou et al. [4]. This can be explained based on the fact that silver addition promotes formation of well-dispersed CuO crystallites, too small to be detected by the XRD technique, or that the concentration of copper was too low. For the catalysts deposited on alumina, silver is present in both metallic and silver oxide form (Ag_2O), while in the case of the catalysts supported on titania there is no metallic silver. For the catalysts supported on titania, silver is present as two different silver oxides—Ag_2O and Ag_2O_3. These different forms of silver result from the different influences of Al_2O_3 and TiO_2. Use of the alumina support promotes formation of reduced silver (Fig. 1), while use of titania allows one to obtain catalysts containing unreduced forms of silver (Fig. 2). In the case of the XRD patterns of the 1.5Cu0.5Ag/Al and 1.5Cu0.5Ag/Ti catalysts, there are no signals from Ag crystallites, probably due to the too low silver content, below the limit of detection.

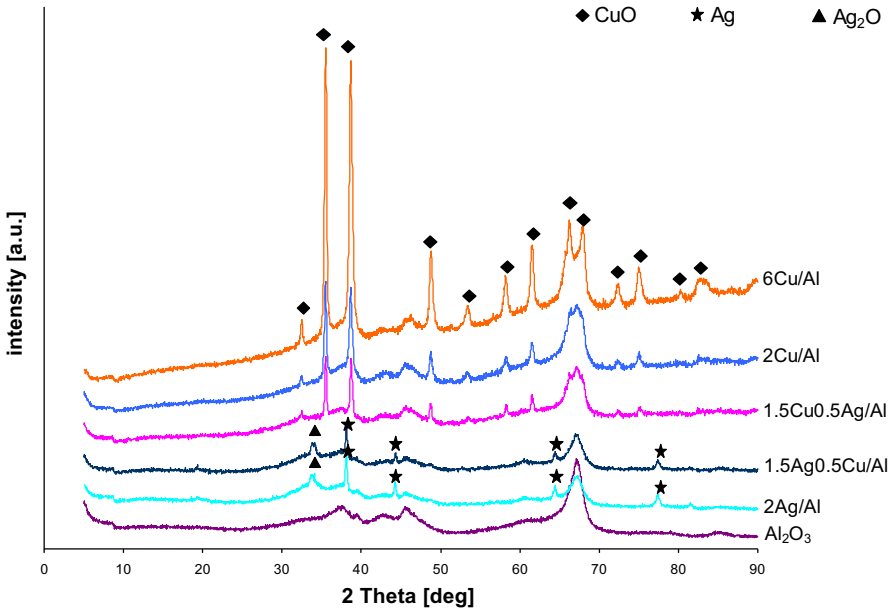

Fig. 1 XRD patterns of CuAg/Al catalysts

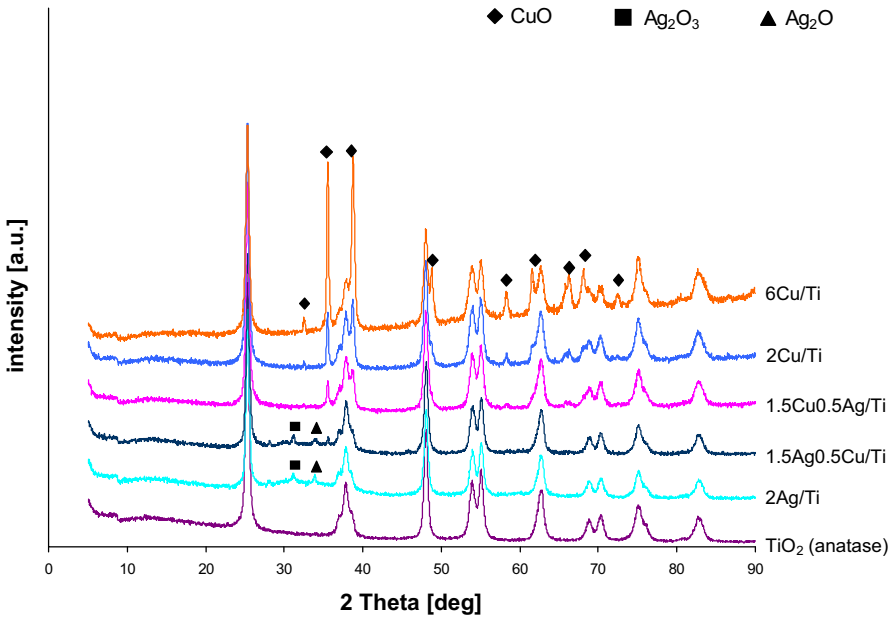

Fig. 2 XRD patterns of CuAg/Ti catalysts

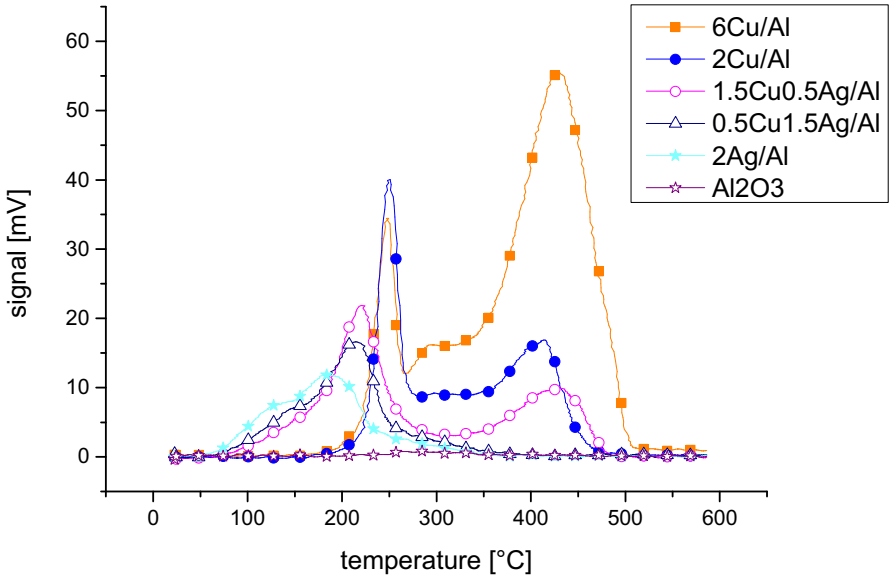

Fig. 3 TPR profiles of CuAg/Al catalysts

Reducibility by TPR-H_2 method

Figures 3 and 4 show the TPR-H_2 profiles of the CuAg/Al and CuAg/Ti catalysts, respectively.

For the samples without silver (6Cu/Al, 6Cu/Ti, 2Cu/Al, and 2Cu/Ti) two reduction peaks, related to reduction of different kinds of copper oxides, are exhibited. The low-temperature peak, with T_{max} at 250 °C for the Al_2O_3 series and 205 °C for the TiO_2 series, corresponds to reduction of smaller copper oxide crystallites or reduction of copper oxide crystallites weakly bonded with the support [17]. Curiously enough, the intensity of this low-temperature peak is almost the same for catalysts containing 2 and 6 mmol of copper, irrespective of the support type. Increasing the copper content in the catalyst leads to an increase of the high-temperature peak (T_{max} at 420 °C for the Al_2O_3 series and 320 °C for the TiO_2 series) intensity, which corresponds to reduction of larger copper oxide crystallites or crystallites that are strongly bonded with the support, being more difficult to reduce. For catalysts containing copper and silver (1.5Cu0.5Ag/Al and 0.5Cu1.5Ag/Al) the first peak is distinctly shifted toward lower temperature, from 250 to 218 °C. This fact suggests that the presence of silver particles facilitates dissociation of a hydrogen molecule, considered the rate-determining step (r.d.s.) of the reduction, as observed previously by Luo et al. [18] for catalysts containing Ag supported on oxides. In the case of the catalyst with low copper content (0.5Cu1.5Ag/Al) there is no high-temperature peak. This means that this sample contains only easily reducible copper oxide. For the catalysts containing only silver phase (2Ag/Al and 2Ag/Ti), the shape of the TPR profiles indicates that there are two kinds of silver oxide, reducible at lower temperature than copper oxide. In the TiO_2

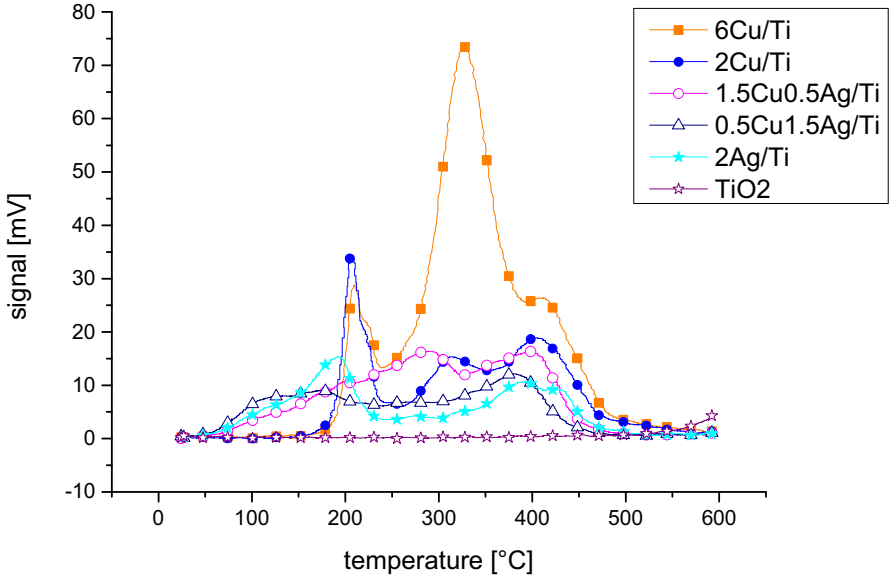

Fig. 4 TPR profiles of CuAg/Ti catalysts

series, the reduction peak with T_{max} at 410 °C is assigned to reduction of the support. As can be seen, the TPR profiles of the catalysts were significantly influenced by the composition of the active phase deposited on the different oxide supports. Both the shifts and intensities indicate that silver addition modifies the redox properties of copper oxide in the studied catalytic systems.

Results of catalytic activity measurements in hydrogenolysis of glycerol

The catalytic behavior of the studied samples in the tested reaction was found to depend on the type of oxide support and the composition of the active CuAg phase. Tables 3 and 4 present the values of glycerol conversion, turnover frequencies (TOF), and selectivities for major products for the CuAg/Al and CuAg/Ti catalysts, respectively. The reaction conditions were the same in all experiments as described in detail in "Catalytic activity measurements" section.

The CuAg/Ti catalysts were found to be more active in the studied reaction than the CuAg/Al ones. The obtained conversions of glycerol for the CuAg/Ti system were between 24 and 47 %, whereas for CuAg/Al they were lower, reaching 38 % at most. Depending on the support used, the main reaction products (with potential industrial application) were also different. In the case of alumina-supported catalysts, the highest selectivities for 1,2-propanediol (1,2-PDO) were obtained for the samples containing only copper phase. For the CuAg/Al samples, 1-propanol and acetol were the predominant products. On the other hand, the CuAg catalysts supported on titania were mainly selective for 1-PO (30–64 %), whereas the selectivities for 1,2-propanediol were low (below 16 %). The highest selectivities for acetol in both series were obtained for the 2Cu and 1.5Cu0.5Ag catalysts. As can be seen, there were distinct differences in the selectivities for 1,2-propanediol between the catalysts containing only active copper phase but supported on the different oxides. Therefore, in this case, the differences in the selectivities are probably caused by differences in the acidity of the studied supports. The 2Ag/Al and 2Ag/Ti catalysts, containing only silver phase, showed the lowest catalytic activity with glycerol conversion of 15 and 24 %, respectively. The main reaction product for both samples was 1-propanol (for

Table 3 Results of catalysis of glycerol hydrogenolysis for CuAg/Al catalysts

Catalyst	Glycerol conversion (%)	TOF[a] (Gly/gMe× h) × 10^{21}	Selectivity for 1,2-PDO (%)	Selectivity for 1-PO (%)	Selectivity for acetol (%)	Other liquid products[b] (%)
6Cu/Al	38	1.73	71	16	4	9
2Cu/Al	36	4.91	54	15	31	0
1.5Cu0.5Ag/Al	16	1.92	0	39	61	0
0.5Cu1.5Ag/Al	20	1.93	11	43	12	34
2Ag/Al	15	1.31	2	93	2	3

Gly number of glycerol molecules; *1,2-PDO* 1,2-propanediol; *1-PO* 1-propanol

[a] TOF calculated on gram of metal (Me wt%), i.e., copper and/or silver

[b] 2-Propanol, ethanol

Table 4 Results of catalysis of glycerol hydrogenolysis for CuAg/Ti catalysts

Catalyst	Glycerol conversion (%)	TOF[a] (Gly/gMe×h) × 10^{21}	Selectivity for 1,2-PDO (%)	Selectivity for 1-PO (%)	Selectivity for acetol (%)	Other liquid products [b] (%)
6Cu/Ti	25	1.14	13	44	10	33
2Cu/Ti	44	6.00	3	62	19	16
1.5Cu0.5Ag/Ti	36	4.31	4	64	13	19
0.5Cu1.5Ag/Ti	47	4.53	7	57	14	22
2Ag/Ti	24	2.09	16	31	2	51

Gly number of glycerol molecules; *1,2-PDO* 1,2-propanediol; *1-PO* 1-propanol

[a] TOF calculated on gram of metal (Me wt %), i.e., copper and/or silver

[b] 2-propanol, ethanol, 2-hydroxyacrolein, glyceraldehydes

2Ag/Al even about 90 %), whereas the selectivities for 1,2-PDO were insignificant. This indicates that dispersed copper is more efficient for glycerol hydrogenolysis reaction than silver, particularly for obtaining desired product such as 1,2-propanediol. Catalysts containing only copper phase are also more active than bimetallic samples; for both supports, the samples denoted 2Cu/Ti and 2Cu/Al were characterized by the highest values of glycerol conversions and TOFs. Depending on the kind of support used, a different distribution of products was observed. In the case of CuAg/Al catalysts, 2-propanol and ethanol were produced in small amounts. These compounds are secondary C–C hydrogenolysis (degradation) products [3] formed via the mechanism described in the "Introduction" [9, 10]. However, 2-hydroxyacrolein and glyceraldehyde were present among the products detected in the catalytic tests carried out with the CuAg/Ti catalysts (Table 4). This indicates that the type of support and its acidity influence the mechanism of the glycerol hydrogenolysis reaction. Another mechanism of glycerol hydrogenolysis, proposed in literature by Montassier et al. [19], suggests glycerol dehydrogenation to glyceraldehyde followed by dehydration to 2-hydroxyacrolein. In this mechanism, 2-hydroxyacrolein is hydrogenated to 1,2-propanediol. Feng et al. [20] found that, for the Ru/TiO_2 system, the pH of the reaction mixture influences the glycerol hydrogenolysis mechanism. They found that a pH increase leads to a change of the hydrogenolysis reaction path to the route via glyceraldehyde. Our results showed that glyceraldehyde and 2-hydroxyacrolein were only obtained for titania-supported catalysts, which is less acidic than alumina, which seems to be in agreement with this mechanism. Further investigation of the acidity of the catalysts will be carried out to determine the correlation between the composition of the active phase supported on the used oxides and the glycerol hydrogenolysis mechanism.

Conclusions

The influence of the support type and the active phase composition was investigated in glycerol hydrogenolysis reaction. It was found that silver addition modifies the redox properties of the catalysts and decreases their specific surface area. The

product distribution and reaction route, in agreement with Scheme 1, depend on the type of support used. Catalysts with high copper content deposited on more acidic alumina allowed achievement of the highest selectivity for 1,2-propanediol (54–71 %) with 36–38 % glycerol conversion. On the other hand, the catalysts supported on less acidic titania were more selective for 1-propanol, which is also an industrially important commodity.

Acknowledgments The authors gratefully acknowledge financial support from the Foundation for Polish Science through project POMOST/2011-3/7 and the Marian Smoluchowski Kraków Research Consortium—a Leading National Research Centre KNOW supported by the Ministry of Science and Higher Education.

References

1. F. Vila, M. López Grandos, M. Ojeda, J.L.G. Fierro, R. Mariscal, Catal. Today **187**, 122–128 (2012)
2. M. Balaraju, K. Jagadeeswaraiah, P.S. Sai Prasad, N. Lingaiah, Catal. Sci. Technol. **2**, 1967–1976 (2012)
3. Y. Nakagawa, K. Tomishige, Catal. Sci. Technol. **1**, 179–190 (2011)
4. J. Zhou, L. Guo, X. Guo, J. Mao, S. Zhang, Green Chem. **12**, 1835–1843 (2010)
5. R.D. Cortright, M. Sanchez-Castillo, J.A. Dumesic, Appl. Catal. B **39**, 353–359 (2002)
6. J. Chaminand, L. Djakovitch, P. Gallezot, P. Marion, C. Pinel, C. Rosier, Green Chem. **6**, 359–361 (2004)
7. M.A. Dasari, P.P. Kiatsimkul, W.R. Sutterlin, G.J. Suppes, Appl. Catal. A **281**, 225–231 (2005)
8. R.B. Mane, A.M. Hengne, A.A. Ghalwadkar, S. Vijayanand, P.H. Mohite, H.S. Potdar, C.V. Rode, Catal. Lett. **135**, 141–147 (2010)
9. M. Balaraju, V. Rekha, P. S. Sai Prasad, Prasa. L. A. Prabhavathi Devi, R. B. N. Prasad, N. Lingaiah, Appl. Catal. A Gen. **354**, 82–87 (2009)
10. Z. Huang, F. Cui, H. Kang, J. Chen, Ch. Xia, Appl. Catal. A Gen. **366**, 288–298 (2009)
11. X. Guo, Y. Li, R. Shi, Q. Liu, E. Zhan, W. Shen, Appl. Catal. A Gen. **371**, 108–113 (2009)
12. M. Balaraju, V. Rekhna, P. S. Sai Prasa, R. B. N. Prasa, N. Lingaiah, Catal. Lett. **126**, 119–124 (2008)
13. J. Zhou, J. Zhang, X. Guo, J. Mao, S. Zhang, Green Chem. **14**, 156–163 (2012)
14. G.J.J. Bartley, R. Burch, R.J. Chappell, Appl. Catal. **43**, 91–104 (1988)
15. K. Sadowska, K. Góra-Marek, J. Datka, Vib. Spectrosc. **63**, 418–425 (2012)
16. J. Słoczyński, R. Grabowski, A. Kozłowska, P. Olszewski, J. Stoch, J. Skrzypek, M. Lachowska, Appl. Catal. A Gen. **278**, 11–23 (2004)
17. J. Słoczyński, R. Grabowski, A. Kozłowska, P. K. Olszewski, J. Stoch, Phys. Chem. Chem. Phys. **5**, 4631–4640 (2003)
18. M. Luo, X. Yuan, X. Zheng, Appl. Catal. A Gen. **175**, 121–129 (1998)
19. C. Montassier, D. Giraud, J. Barber, Stud. Surf. Sci. Catal. **41**, 165–170 (1988)
20. J. Feng, J. Wang, Y. Yhou, H. Fu, H. Chen, X. Li, Chem. Lett. **36**(10), 1274–1275 (2007)